Wave Motion 113 (2022) 102977

Contents lists available at ScienceDirect

Wave Motion

journal homepage: www.elsevier.com/locate/wamot

Implementation of Deutsch and Deutsch–Jozsa-like algorithms involving classical entanglement of elastic bits

Pierre A. Deymier [*,1], Keith Runge [1], M. Arif Hasan [1]

Department of Materials Science and Engineering, University of Arizona, Tucson AZ 85721, United States of America

ARTICLE INFO

Article history:
Received 29 April 2021
Received in revised form 13 August 2021
Accepted 9 June 2022
Available online 18 June 2022

Keywords:
Elastic waves
Elastic bit
Quantum-like algorithm
Nonseparable waves
Classical entanglement

ABSTRACT

We present the implementation of two quantum-like algorithms which exploit classical entanglement (i.e., nonseparability) of elastic waves. The Deutsch–Jozsa-like algorithm can distinguish between the even or odd character of all possible binary functions for two elastic bits inputs. The Deutsch-like algorithm distinguishes between constant and balance binary functions also using two elastic bits. These algorithms can be implemented on simple elastic systems composed of a planar array of two finite one-dimensional discrete elastic waveguides mutually coupled periodically along their length and driven externally.

1. Introduction

Human speech uses sound waves as analog signal to encode and convey information. Acoustic cues such as frequency and amplitude modulations allow communicators to derive meaning. However, today, most information encoding, transmission and processing techniques are carried out in the digital domain where signaling cues are restricted to some discrete set of values. Modern digital information processing machines are built from electronic digital logic circuits whose elementary units are Boolean logic gates. They use the binary numbers 0 and 1 to implement Boolean functions such as the NOT, AND, OR gates. It is desirable to consider information processing techniques relying on all mechanical integrated circuits for energy efficiency. Mechanical information processing platforms have been suggested for traditional digital operations using non-linear interactions [1]. The development of phononic crystals and acoustic metamaterials has also provided physical platforms for the realization of acoustic Boolean logic gates. By exploiting the unique spectral, refractive and phase properties of some phononic crystals one can achieve constructive or destructive interference between input and control acoustic waves to achieve Boolean functions [2]. Similarly, interferences have been used to demonstrate Boolean logic gates in acoustic metamaterials [3]. Interference-based gating relies on the linear behavior of the acoustic waves. Acoustic logic elements have also been demonstrated in driven chains of spherical particles [4,5]. These gates exploit the nonlinear dynamical effects associated with the contact forces between spheres.

Moreover, the analogies between classical wave physics and quantum mechanics offer avenues to go beyond Boolean logic to pursue sound-based information processing that emulate quantum-like computing functionalities. In contrast to conventional computing, where a bit can be in a 0 or 1 state, quantum computing processes coherent superposition of states. A quantum computer uses quantum bits, or qubits. Qubit-based computing platforms capitalize on the phenomenon

* Corresponding author.
E-mail addresses: deymier@arizona.edu (P.A. Deymier), krunge@arizona.edu (K. Runge), mdhasan@arizona.edu (M.A. Hasan).

[1] All authors contributed equally to the research reported in this article and to the writing to the article.

https://doi.org/10.1016/j.wavemoti.2022.102977
0165-2125/

of superposition, which allows a quantum computer to simultaneously process information beyond that achievable with electronic transistor-based processors. A qubit is a two-state (level) quantum-mechanical system, such as an electron in which the levels can be taken as spin up (0) and spin down (1). Another example is the polarization of a single photon in which the two states can be taken to be the vertical polarization (0) and the horizontal polarization (1). An electron spin qubit can be in a coherent superposition of spin up or down. A single photon can be in a superposition of vertical and horizontal polarization. Superposition is essentially the ability of a system to be in multiple states—that is a qubit can store and process a "0" and a "1" at the same time. Furthermore, quantum computers harness strong quantum correlations between qubits (also known as entanglement) to achieve massive-data information processing. Entangled qubits are inseparable, that is the state of each entangled qubit cannot be described separately from that of the other qubits. Manipulation of the state of one qubit affects the state of the other qubits. Entanglement is at the core of today's second quantum revolution [6]. Quantum algorithms harness entanglement to speed up computational tasks beyond what can be achieved with classical computers [7].

The similarity between the equations governing quantum mechanics and classical waves have been exploited to illustrate quantum phenomena. Metamaterials which can simulate quantum algorithms such as the Deutsch/Deutsch–Jozsa or Grover's search algorithms with classical light have been reported [8–13]. However, these simulations rely on wave superposition and interference as both class of algorithms for two bits do not need entanglement. While nonlocality of entangled states is a unique feature of quantum mechanics, nonseparability is not. The notion of "classical entanglement", i.e., local nonseparable superposition of states has received a significant amount of attention, theoretically and experimentally in optics [14–20]. Recent work in the field of acoustics, has demonstrated the possibility of creating "classically entangled" elastic waves. For instance, externally driven parallel arrays of coupled metallic elastic waveguides enabled preparation and tunability of acoustic nonseparable states, i.e., Bell states, supported by coupled elastic waveguides [21]. These nonseparable states, are analogous to "entangled" states of qubits and are constructed as a superposition of elastic waves, each a tensor product of a spinor part and an orbital angular momentum part, which cannot be factored as a single tensor product. The concept of classical entanglement was also demonstrated in elastic analogues of nonseparable qutrits, the three-level equivalent of the two-level qubit [22]. These nonseparable superpositions of acoustic states possess complex amplitude coefficients which can be tuned to navigate a sizeable portion of the Bell state's Hilbert space enabling quantum-like operations. The possibility of achieving maximally entangled exponentially complex superpositions was also shown in nonlinear product states supported by externally driven arrays of nonlinear waveguides [23]. Finally, a planar array of three one-dimensional elastic waveguides mutually coupled periodically along their length and driven externally was shown theoretically and numerically to support expansive nonseparable superpositions of product states representative of a bipartite system composed of two subsystems. These states are the product of Bloch waves describing the elastic displacement along the waveguides (states of subsystem 1) and spatial modes representing the displacement across the array of waveguides (states of subsystem 2) [24]. The periodicity of the coupling was used to fold bands enabling superpositions of states that span the complete Hilbert space of product states. The bipartite system is analogous to two bits if we chose $|e_i\rangle$, i=1,2, to be two discrete spatial modes of the subsystem 1 and by $|k_j\rangle$, j=1,2, two discrete plane wave components of the Bloch modes of the subsystem 2. Indeed, externally driven periodically coupled arrays of elastic waveguides can sustain general superposition of product states: $A\,|e_1\rangle\,|k_1\rangle + B\,|e_1\rangle\,|k_2\rangle + C\,|e_2\rangle\,|k_1\rangle + D\,|e_2\rangle\,|k_2\rangle$. Here, the coefficients A, B, C and D are effectively complex resonant amplitudes when the driven elastic system is dissipative. By tuning the physical and/or geometrical attributes of the system as well as by varying the characteristics of the external driver, one can explore a sizeable region of the Hilbert space of product elastic states. Manipulation of such a superposition of product states allows the creation of non-separable Bell states of the form: $A\,|e_1\rangle\,|k_1\rangle + D\,|e_2\rangle\,|k_2\rangle$ or $B\,|e_1\rangle\,|k_2\rangle + C\,|e_2\rangle\,|k_1\rangle$ or separable states that can be factored in the form $(a\,|e_1\rangle + b\,|e_2\rangle)\,(c\,|k_1\rangle + d\,|k_2\rangle)$.

It is the objective of the present study to show that band folding within a finite Brillouin zone due to periodic coupling between two elastic waveguides offers the possibility of creating superpositions of product states that can be tuned between separable and nonseparable forms by stimulating the system externally with an oscillatory driver. This freedom can be used to implement a Deutsch and Deutsch–Jozsa-like algorithm involving classical entanglement of two elastic bits. More specifically, these algorithms, are shown to distinguish between the even/odd or constant/balanced character of binary functions for elastic bits inputs.

The paper is organized as follows. In Section 2, we introduce the model constituted of two one-dimensional discrete elastic waveguides mutually coupled periodically along their length. We detail the decomposition of the elastic modes into products of spatial modes across the waveguides and Bloch modes along the waveguides. Section 3 highlights the creation of superpositions of product states by driving the periodically coupled elastic waveguides externally. The navigation of the Hilbert space of the bipartite system between separable and nonseparable states by tuning the driver's frequency is described in Section 4. We exploit the tunability of the separability of superpositions of product states to implement a Deutsch–Jozsa-like algorithm that requires classical entanglement. This algorithm distinguishes between the even or odd character of all possible binary functions of two bits by utilizing a controlled Z gate unitary transformation as its primary operation. In Section 6, we show how to achieve a controlled NOT (CX) gate and implement a Deutsch-like algorithm to distinguish between constant and balanced binary functions. Conclusions concerning the applicability, scalability and extension of this work to other elastic systems that support nonseparable superpositions and to other quantum-like algorithms are drawn in Section 7.

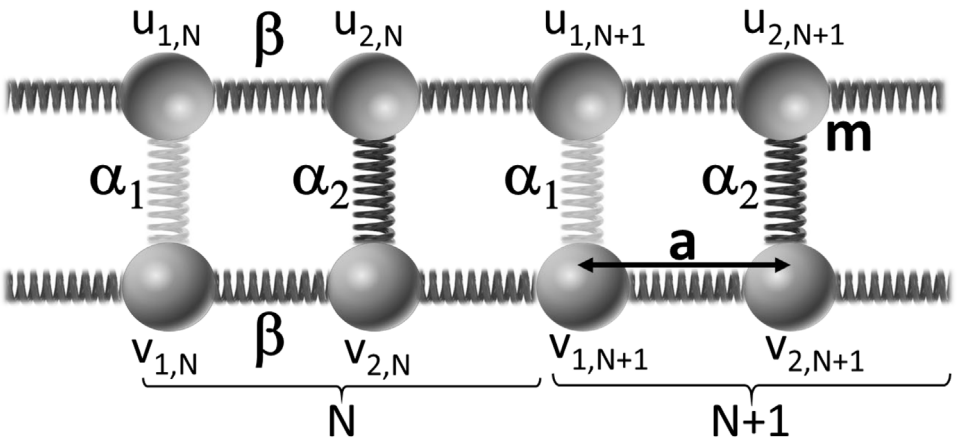

Fig. 1. Schematic representation of the model system composed of two discrete elastic waveguides coupled periodically along their length. See text for definition of symbols.

2. One-dimensional elastic waveguides mutually coupled periodically along their length

The model system is initially constituted of two identical infinite discrete elastic waveguides taking the form of harmonic chains with mass, m, and spring stiffness, β. The two chains are coupled elastically along their length via springs with alternating stiffness, α_1 and α_2. The system is therefore periodic with period, $L = 2a$ where a is the inter-mass spacing. Units cells along the coupled waveguides are labeled, N, $N+1$, etc (see Fig. 1) .

The equations of motion of this system are given below:

$$m\frac{\partial^2 u_{1,N}}{\partial t^2} = \beta\left(u_{2,N-1} - 2u_{1,N} + u_{2,N}\right) + \alpha_1\left(v_{1,N} - u_{1,N}\right) \tag{1a}$$

$$m\frac{\partial^2 u_{2,N}}{\partial t^2} = \beta\left(u_{1,N} - 2u_{2,N} + u_{1,N+1}\right) + \alpha_2\left(v_{2,N} - u_{2,N}\right) \tag{1b}$$

$$m\frac{\partial^2 v_{1,N}}{\partial t^2} = \beta\left(v_{2,N-1} - 2v_{1,N} + v_{2,N}\right) - \alpha_1\left(v_{1,N} - u_{1,N}\right) \tag{1c}$$

$$m\frac{\partial^2 v_{2,N}}{\partial t^2} = \beta\left(v_{1,N} - 2v_{2,N} + v_{1,N+1}\right) - \alpha_2\left(v_{2,N} - u_{2,N}\right) \tag{1d}$$

In Eq. (1a,b,c,d), u and v represent the displacement in the top and bottom chains, respectively.

To solve these equations of motion, we use the ansatz, $\vec{U}_N = \begin{pmatrix} u_{1,N} \\ u_{2,N} \\ v_{1,N} \\ v_{2,N} \end{pmatrix} = \vec{A}e^{ikNL}e^{i\omega t}$ with the amplitude vector $\vec{A} = \begin{pmatrix} A_1 \\ A_2 \\ B_1 \\ B_2 \end{pmatrix}$. k and ω are a wave number and angular frequency. Inserting this ansatz into Eq. (1a,b,c,d) and after some factorization, one obtains:

$$\left(\overleftrightarrow{M} \otimes \overleftrightarrow{I}_2 + \overleftrightarrow{\alpha} \otimes \overleftrightarrow{c}\right)\vec{A} = 0 \tag{2}$$

where $\overleftrightarrow{M} = \begin{pmatrix} \gamma & -\delta^* \\ -\delta & \gamma \end{pmatrix}$, $\overleftrightarrow{I}_2$ is the 2×2 identity matrix, $\overleftrightarrow{\alpha} = \begin{pmatrix} \alpha_1 & 0 \\ 0 & \alpha_2 \end{pmatrix}$ and $\overleftrightarrow{c} = \begin{pmatrix} 1 & -1 \\ -1 & 1 \end{pmatrix}$. Here $\gamma = -m\omega^2 + 2\beta$, $\delta = \beta\left(1 + e^{ikL}\right)$ and δ^* is its complex conjugate. The form of Eq. (2) suggests solutions of the form of tensor products: $\vec{A} = \vec{s}_n \otimes \vec{e}_n$ where $\vec{e}_n$ is an Eigen vector of the coupling matrix $\overleftrightarrow{c}$. The spatial Eigen vectors $\vec{e}_n$ represent the displacement across the array of waveguides. The Eigen values and vectors of $\overleftrightarrow{c}$ are: $\lambda_1 = 0$, $\vec{e}_1 = \frac{1}{\sqrt{2}}\begin{pmatrix} 1 \\ 1 \end{pmatrix}$ and $\lambda_2 = 2$, $\vec{e}_2 = \frac{1}{\sqrt{2}}\begin{pmatrix} -1 \\ 1 \end{pmatrix}$. $\vec{s}_n$ is a 2×1 vector.

With these, Eq. (2) yields:

$$\left(\overleftrightarrow{M} + \lambda_n \overleftrightarrow{\alpha}\right)\vec{s}_n = 0 \tag{3}$$

Nontrivial solutions exist if $det\left(\overleftrightarrow{M} + \lambda_n \overleftrightarrow{\alpha}\right) = 0$, i.e.,

$$(\gamma + \lambda_n\alpha_1)(\gamma + \lambda_n\alpha_2) - \delta\delta^* = 0 \tag{4}$$

The dispersion relations for the two possible values of n are

$$m\omega_1^2(k) = 2\beta\left(1 \pm \left|\cos\frac{kL}{2}\right|\right) \tag{5a}$$

$$m\omega_2^2(k) = 2\beta + \alpha_1 + \alpha_2 \pm \sqrt{(\alpha_1 - \alpha_2)^2 + 4\beta^2\cos^2\frac{kL}{2}} \tag{5b}$$

We now consider that the coupled system is composed of finite waveguides. Let N_c be the number of unit cells along the waveguides. The cell index N now runs over the finite set $0, 1, 2, 3, \ldots, N_c - 1$. The waveguides are arranged in a loop manner by imposing periodic boundary conditions, that is, $\vec{U}_{N_c} = \vec{U}_0$ or $e^{ikN_cL} = 1$. The wave number is now discrete with $k_j = \frac{2\pi}{N_cL}j$ with $j = 0, 1, 2, 3, \ldots, N_c - 1$. In Fig. 2(A), we illustrate the dispersion relations given by Eq. ((5)a,b) for a finite system composed of 10 units cells. The physical and geometrical parameters are listed in the caption of Fig. 2.

The band structure can be tuned by varying the physical parameters of the system m, β, α_1, α_2 but also the geometrical parameter N_c. In Fig. 2, we have chosen a combination of parameters such that the $n = 1$ upper band crosses the bottom $n = 2$ band. These parameters also lead to an intersection flanked by four modes. This intersection is made possible by the folding of the $n = 1$ band resulting from the periodicity of the coupling between the two chains. The "a" ($n = 1$) and "c" ($n = 2$) modes correspond to different Eigen vectors $\vec{e}_n$ but possess the same wave number k. The "b" ($n = 1$) and "d" ($n = 2$) modes also represent the different Eigen vectors $\vec{e}_n$ but now possess the same wave number k'. This particular configuration will enable the creation of externally driven nonseparable superpositions of states discussed in the next section.

3. Externally driven periodically coupled elastic waveguides

Eq. ((1)a,b,c,d) (limited to the finite size waveguides) are now augmented by an external force $\vec{F} = \vec{D}\delta_{N=0}e^{i\omega_D t}$ with amplitude $\vec{D} = \begin{pmatrix} F_1 \\ F_2 \\ G_1 \\ G_2 \end{pmatrix}$. Here, $\delta_{N=0}$ is the Dirac delta function that enforces that the external driver is applied onto the $N = 0$ unit cell. ω_D is the angular frequency of the external driver. We seek solutions as superpositions over available wave numbers, $\vec{U}_N^D = \sum_{j=0}^{N_c-1}\vec{A}_D(k_j)e^{ik_jNL}e^{i\omega_D t}$ with the driven amplitude vector $\vec{A}_D = \begin{pmatrix} A_{1,D} \\ A_{2,D} \\ B_{1,D} \\ B_{2,D} \end{pmatrix}$. We also expand the Dirac delta function as a Riemann sum over the same available wave numbers, namely $\delta_{N=0} = \frac{1}{N_c}\sum_{j=0}^{N_c-1}e^{ik_jNL}$. Inserting these expressions in the equations of motion of the driven system for each k_j, leads to:

$$\left(\overleftrightarrow{M}_D \otimes \overleftrightarrow{I}_2 + \overleftrightarrow{\alpha} \otimes \overleftrightarrow{c}\right)\vec{A}_D(k_j) = \vec{D} \tag{6}$$

In Eq. (6), $\overleftrightarrow{M}_D$ takes the same form as $\overleftrightarrow{M}$ in the previous section but with γ replaced by $\gamma_D = -m\omega_D^2 + 2\beta$.

Since $\vec{e}_1$ and $\vec{e}_2$ form a complete orthonormal basis, we can expand $\vec{D}$ as

$$\vec{D} = \vec{f}\vec{e}_1 + \vec{g}\vec{e}_2 \tag{7}$$

where $\vec{f} = \begin{pmatrix} f_1 \\ f_2 \end{pmatrix}$ and $\vec{g} = \begin{pmatrix} g_1 \\ g_2 \end{pmatrix}$ with $f_1 = \frac{F_1+G_1}{\sqrt{2}}$, $f_2 = \frac{F_2+G_2}{\sqrt{2}}$, $g_1 = \frac{F_1-G_1}{\sqrt{2}}$, and $g_2 = \frac{F_2-G_2}{\sqrt{2}}$.

Within that same basis, we seek driven solutions given by:

$$\vec{A}_D(k_j) = \vec{S}_1^D(k_j) \otimes \vec{e}_1 + \vec{S}_2^D(k_j) \otimes \vec{e}_2 \tag{8}$$

Inserting Eqs. (7) and (8) into Eq. (5) results in the set of equations:

$$\left(\overleftrightarrow{M}_D + \lambda_1\overleftrightarrow{\alpha}\right)\vec{S}_1^D(k_j) = \vec{f} \tag{9a}$$

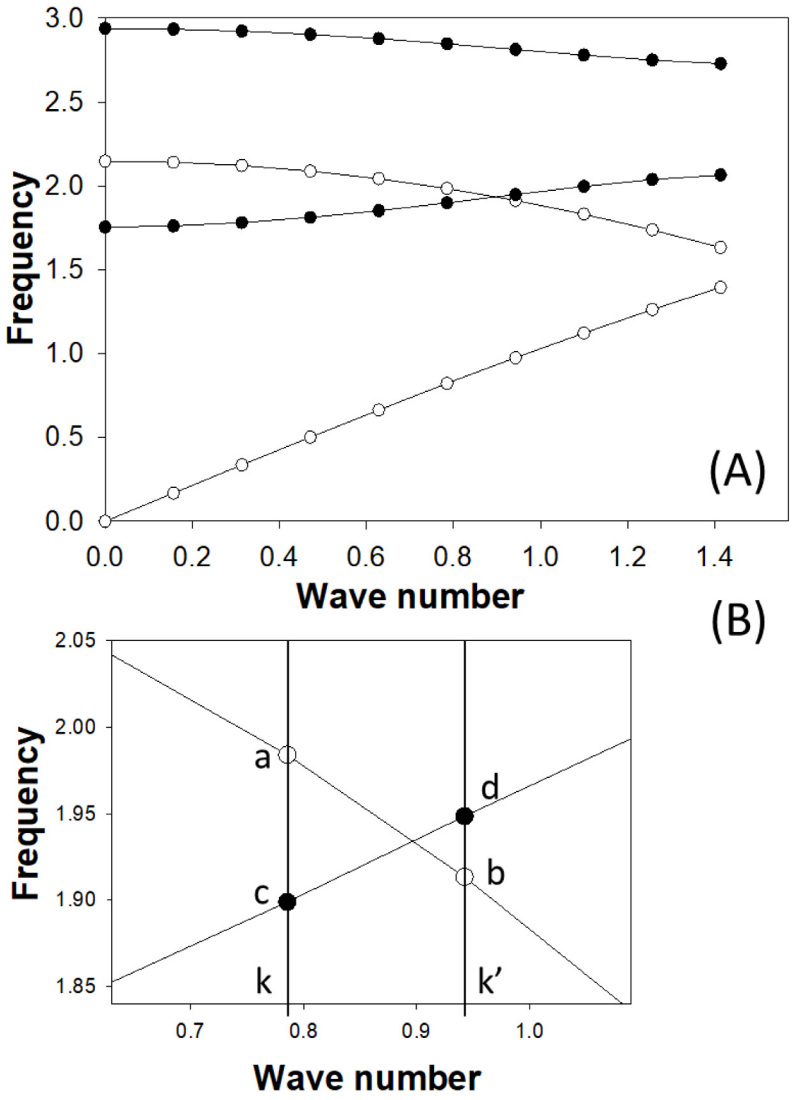

Fig. 2. (A) Band structure of the coupled finite length waveguides. The open circles represent the bands $\omega_1^{\pm}(k)$ and the closed circles the bands $\omega_2^{\pm}(k)$. We have chosen the dimensionless parameters $m = 1$, $\beta = 1.153$, $\alpha_1 = 1$, $\alpha_2 = 2.55$, and $N_c = 10$, such that the top open circle band intersects the bottom closed circle band. (B) magnified region with band intersection. Note that the modes labeled "a" and "c" have the same wave number k. "b" and "d" correspond to modes with the same wave number k'.

$$\left(\overleftrightarrow{M}_D + \lambda_2 \overleftrightarrow{\alpha}\right) \vec{S}_2^D\left(k_j\right) = \vec{g} \tag{9b}$$

Solutions of Eqs. ((9) a,b) take the form

$$S_{1,1}^D\left(k_j\right) = \frac{\gamma_D f_1 + \delta^* f_2}{\gamma_D^2 - \gamma_1^2} \tag{10a}$$

$$S_{2,1}^D\left(k_j\right) = \frac{\delta f_1 + \gamma_D f_2}{\gamma_D^2 - \gamma_1^2} \tag{10b}$$

$$S_{1,2}^D\left(k_j\right) = \frac{\left(\gamma_D + 2\alpha_2\right) g_1 + \delta^* g_2}{\left(\gamma_D + 2\alpha_1\right)\left(\gamma_D + 2\alpha_2\right) - \left(\gamma_2 + 2\alpha_1\right)\left(\gamma_2 + 2\alpha_2\right)} \tag{10c}$$

$$S_{2,2}^D\left(k_j\right) = \frac{\delta g_1 + \left(\gamma_D + 2\alpha_1\right) g_2}{\left(\gamma_D + 2\alpha_1\right)\left(\gamma_D + 2\alpha_2\right) - \left(\gamma_2 + 2\alpha_1\right)\left(\gamma_2 + 2\alpha_2\right)} \tag{10d}$$

In Eqs. ((10)a,b,c,d), we have use $S^D_{1,1}$ and $S^D_{2,1}$ to denote the two components of the vector $\vec{S}^D_1$. Similarly, $S^D_{1,2}$ and $S^D_{2,2}$ stand for the components of $\vec{S}^D_2$. Here, γ_1 and γ_2 are the γ's solutions of Eq. (4) for $n = 1,2$.

In the presence of dissipation, we add to the equations of motion terms of the form $-\mu\frac{\partial}{\partial t}$. μ is a dissipation coefficient. In that case, γ_D becomes complex and $\gamma_D = -m\omega_D^2 + 2\beta - i\mu\omega_D$.

In summary, the displacement field in the externally driven coupled finite waveguide system is

$$\vec{U}^D_N = \sum_{j=0}^{N_c-1}\left(\vec{S}^D_1\left(k_j\right)\otimes\vec{e}_1 + \vec{S}^D_2\left(k_j\right)\otimes\vec{e}_2\right)e^{ik_jNL}e^{i\omega_D t} \tag{11}$$

With the components of $\vec{S}^D_1$ and $\vec{S}^D_2$ given by Eqs. (10). If we expand these two vectors on the complete orthonormal basis $\vec{x} = \begin{pmatrix}1\\0\end{pmatrix}$ and $\vec{y} = \begin{pmatrix}0\\1\end{pmatrix}$, Eq. (11) can be reformulated as

$$\vec{U}^D_N = \sum_{j=0}^{N_c-1}\left(S^D_{1,1}\vec{x}\otimes\vec{e}_1 + S^D_{1,2}\vec{x}\otimes\vec{e}_2 + S^D_{2,1}\vec{y}\otimes\vec{e}_1 + S^D_{2,2}\vec{y}\otimes\vec{e}_2\right)e^{ik_jNL}e^{i\omega_D t} \tag{12}$$

The external driver creates a coherent superposition of elastic states. By changing the driving frequency, we can change the superposition of states.

If we now consider that the driving frequency is chosen in the vicinity of the band intersection of Fig. 2(B), and using the fact that the components $S^D_{1,1}$, $S^D_{2,1}$, $S^D_{1,2}$, and $S^D_{2,2}$ are resonant terms, we can approximate Eq. (12) by restrict the summation over the available wave numbers to the two dominant wave numbers k and k'. In that case, the displacement field reduces to

$$\begin{aligned}\vec{U}^D_N = \big(&S^D_{1,1}(k)\vec{x}\otimes\vec{e}_1e^{ikNL} + S^D_{1,2}(k)\vec{x}\otimes\vec{e}_2e^{ikNL} + S^D_{2,1}(k)\vec{y}\otimes\vec{e}_1e^{ikNL} + S^D_{2,2}(k)\vec{y}\otimes\vec{e}_2e^{ikNL}\\ &+ S^D_{1,1}\left(k'\right)\vec{x}\otimes\vec{e}_1e^{ik'NL} + S^D_{1,2}\left(k'\right)\vec{x}\otimes\vec{e}_2e^{ik'NL} + S^D_{2,1}\left(k'\right)\vec{y}\otimes\vec{e}_1e^{ik'NL}S^D_{2,2}\left(k'\right)\vec{y}\otimes\vec{e}_2e^{ik'NL}\big)e^{i\omega_D t}\end{aligned} \tag{13}$$

In other words, we are driving near resonance a subset of near-degenerate modes so that a small subspace of vibrations is suitable for describing the state of the much larger number of modes.

Here, the 8 terms $\vec{x}\otimes\vec{e}_1e^{ikNL}$, $\vec{x}\otimes\vec{e}_2e^{ikNL}$, $\vec{y}\otimes\vec{e}_1e^{ikNL}$, $\vec{y}\otimes\vec{e}_2e^{ikNL}$, $\vec{x}\otimes\vec{e}_1e^{ik'NL}$, $\vec{x}\otimes\vec{e}_2e^{ik'NL}$, $\vec{y}\otimes\vec{e}_1e^{ik'NL}$, $\vec{y}\otimes\vec{e}_2e^{ik'NL}$ form the basis of a 2^3 dimensional Hilbert space $H = H_1\otimes H_2\otimes H_3$, tensor product of three 2D Hilbert spaces. H_1 is the Hilbert space associated with the sites in a unit cell with basis $\left\{\vec{x},\vec{y}\right\}$. H_2 is the space associated with degrees of freedom across the coupled chains with basis $\left\{\vec{e}_1,\vec{e}_2\right\}$. H_3 represents degrees of freedom along the waveguides labeled by the wave numbers k and k' with basis functions $\left\{e^{ikNL}, e^{ik'NL}\right\}$. Each one of these two-level subsystems represents an elastic bit. Eq. (13) consists of a superposition of product states of three two-level elastic bits with complex amplitude components. This superposition of states is not separable (classically entangled) if it cannot be written as a product $\left(X\vec{x}+Y\vec{y}\right)\otimes\left(E_1\vec{e}_1+E_2\vec{e}_2\right)\left(Ke^{ikNL}+K'e^{ik'NL}\right)$ with X, Y, E_1, E_2, K and K' complex coefficients. By varying the driving frequency ω_D one can "rotate" the superposition of state by tuning the complex amplitude components, $S^D_{1,1}$, $S^D_{2,1}$, $S^D_{1,2}$, and $S^D_{2,2}$. The extent of such a rotation in the Hilbert space H is dictated by the physical system.

4. Nonseparable superpositions of elastic states in coupled waveguides

We investigate Eq. (13) further by considering that measurements of the displacement field are performed on the first site of the Nth unit cell. This condition reduces the expression for the displacement field to the $\vec{x}$ terms only in Eq. (13). We denote this displacement field, $\vec{V}^D_N$ and write

$$\vec{V}^D_N = \left(S^D_{1,1}(k)\vec{e}_1e^{ikNL} + S^D_{1,1}\left(k'\right)\vec{e}_1e^{ik'NL} + S^D_{1,2}(k)\vec{e}_2e^{ikNL} + S^D_{1,2}\left(k'\right)\vec{e}_2e^{ik'NL}\right)e^{i\omega_D t} \tag{14}$$

The sum of terms in the parenthesis is now a superposition of states in the 2^2-dimensional Hilbert subspace: $H_{sub} = H_2\otimes H_3$. Controlling the driving frequency ω_D enables us to navigate that subspace within some range dictated by the physical system. The operation being performed on the coupled waveguides through the action of changing the external driving frequency, is a process that is agnostic to the state it is being performed on.

To simplify our argument, we choose a driving force such that $f_1 = g_1 = 0$ and $f_2 = g_2 = 1$. This is equivalent to driving the second mass in the top chains in the 0th unit cell. In this case, the complex amplitudes are rewritten as

$$S^D_{1,1}(k,\omega_a) = \frac{\delta^*(k)}{\gamma_D^2 - \gamma_1^2(\omega_a)} \tag{15a}$$

$$S^D_{1,1}\left(k',\omega_b\right) = \frac{\delta^*(k')}{\gamma_D^2 - \gamma_1^2(\omega_b)} \tag{15b}$$

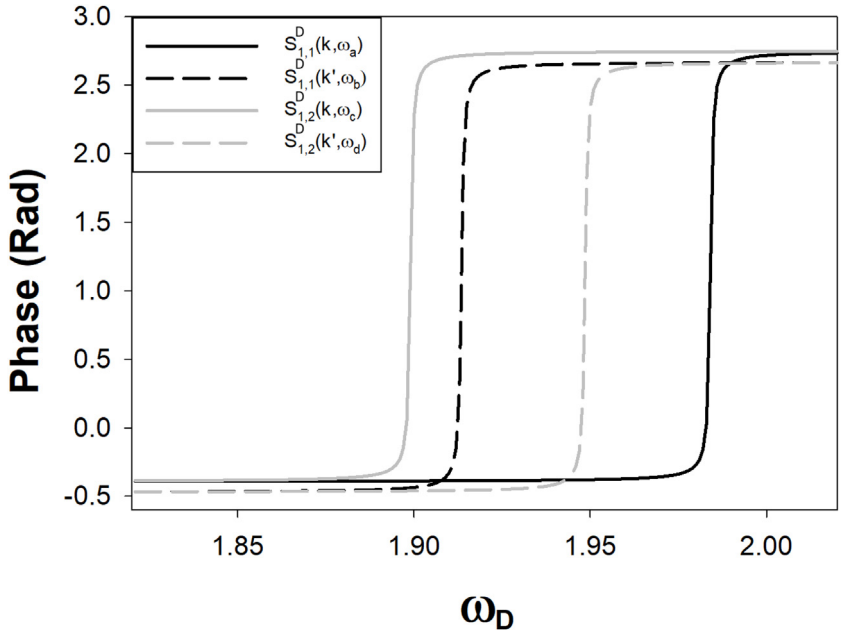

Fig. 3. Phase of the complex amplitudes Eqs. ((15)a,b,c,d)) as functions of the driving frequency. We have chosen $m = 1$, $\beta = 1.153$, $\alpha_1 = 1$, $\alpha_2 = 2.55$, $N_c = 10$, and a dissipation coefficient $\mu = 0.001$. We recall as illustrated in Fig. 2(B), that the modes labeled "a" and "c" have the same wave number k (solid lines). "b" and "d" correspond to modes with the same wave number k' (dashed lines).

$$S^D_{1,2}(k,\omega_c) = \frac{\delta^*(k)}{(\gamma_D + 2\alpha_1)(\gamma_D + 2\alpha_2) - (\gamma_2(\omega_c) + 2\alpha_1)(\gamma_2(\omega_c) + 2\alpha_2)} \tag{15c}$$

$$S^D_{1,2}(k',\omega_d) = \frac{\delta^*(k')}{(\gamma_D + 2\alpha_1)(\gamma_D + 2\alpha_2) - (\gamma_2(\omega_d) + 2\alpha_1)(\gamma_2(\omega_d) + 2\alpha_2)} \tag{15d}$$

In Eqs. ((15)a,b,c,d), we have added for clarity the full dependency on wave numbers and frequencies.

Using the numerical values corresponding to Fig. 2(B), $k = 0.7854$, $k' = 0.9425$, $\omega_a = 1.9841$, $\omega_b = 1.9135$, $\omega_c = 1.8990$ and $\omega_d = 1.9486$, we have plotted in Fig. 3 the argument (phase) of the complex amplitudes Eqs. ((15)a,b,c,d) as functions of the driving frequency ω_D.

The phase of the complex amplitudes takes the usual form of a resonance. The change in phase across each resonance is nearly π. It is not exactly π because of the small additional phase arising from $\delta^*(k)$ and $\delta^*(k')$. The ordering of the resonances, $S^D_{1,2}(k,\omega_c)$, $S^D_{1,1}(k',\omega_b)$ $S^D_{1,2}(k',\omega_d)$, and $S^D_{1,1}(k,\omega_a)$ follows the arrangement of the a, b, c, and d modes in order of increasing frequencies ω_c, ω_b, ω_d, and ω_a.

Let us define $\varphi_1 = \arg\left(S^D_{1,1}(k,\omega_a)\right)$, $\varphi_2 = \arg\left(S^D_{1,1}(k',\omega_b)\right)$, $\varphi_3 = \arg\left(S^D_{1,2}(k,\omega_c)\right)$, and $\varphi_4 = \arg\left(S^D_{1,2}(k',\omega_d)\right)$.

We now construct a state vector, $\vec{W}$, that also lies in a 2^2 dimensional Hilbert space related to H_{sub}:

$$\vec{W}(\omega_D) = \begin{pmatrix} e^{i\Delta\varphi_1} \\ e^{i\Delta\varphi_2} \\ e^{i\Delta\varphi_3} \\ e^{i\Delta\varphi_4} \end{pmatrix}$$ where $\Delta\varphi_l = \varphi_l(\omega_D) - \varphi_l(\omega_D = 1.85)$, $l = 1, 2, 3, 4$. Since the phases $\varphi_l(\omega_D = 1.85)$ are all very close to each other, we effectively refer the argument of the complex amplitude to a general phase.

In Eq. (14), we "partitioned" the system between the spatial degrees of freedom across and along the waveguides. However, the partitioning of the Hilbert space of a physical system into subsystems is not unique and may be dictated by the resources available to access and manipulate its degrees of freedom [25,26]. Therefore, Eq. (14) is but one possible representation of the state of the system. Since the notion of classical entanglement (i.e., nonseparability) is relative to a choice of representation, we have chosen a representation which leads to bipartite states based on phases. The normalized components of $\vec{W}$ form the complex coefficients of a linear combination of 2^2 dimensional tensor product basis vectors. Eqs. (14) and ((15)a,b,c,d) show that the phase differences $\Delta\varphi_{1,2,3,4}$ are expressible in terms of good "quantum" numbers, namely the two "n" labeling the spatial Eigen vectors $\vec{e}_n$ and the associated discrete sets of wave numbers, k and k'. Any representation $\vec{W}$ of the elastic state of the system, $\vec{V}^D_N$, that is a function of the $\Delta\varphi_{1,2,3,4}$ is therefore expressible in terms of these "quantum" numbers. For the given representation, $\vec{W}$, there will exist a tensor product structure and tensor product

basis in which it can be expanded which is also expressible in terms of $\vec{e}_n$ and k and k'. We use this representation for subsequent nonseparability-based information processing.

For $\omega_D \sim 1.92$, $\vec{W}$ is approximately $\begin{pmatrix} 1 \\ -1 \\ -1 \\ 1 \end{pmatrix} = \begin{pmatrix} 1 \\ -1 \end{pmatrix} \otimes \begin{pmatrix} 1 \\ -1 \end{pmatrix}$. This vector could also be obtained by listing the sign of the $e^{i\Delta\varphi_l}$, $l = 1, 2, 3, 4$. This is a separable state as $\vec{W}$ can be written as a tensor product of two 2×1 vectors. In contrast, $\vec{W}$ ($\omega_D \sim 1.96$) is approximately $\begin{pmatrix} 1 \\ -1 \\ -1 \\ -1 \end{pmatrix}$. This vector cannot be factored as a tensor product hence this state is nonseparable. As we continue to increase the driving frequency, we see that $\vec{W}$ ($\omega_D > 2.0$) $= \begin{pmatrix} -1 \\ -1 \\ -1 \\ -1 \end{pmatrix}$ which is fully separable. The ability to tune the separability or nonseparability of the displacement field is a critical property of the coupled waveguide systems that enables the development of algorithms analogous to quantum algorithm. An example is given in the next section.

5. Implementation of Deutsch–J ozsa-like algorithm exploiting classically entangled elastic states

Here, we develop a two-bit algorithm, in the same vein as the Deutsch–Jozsa algorithm [27], that involves nonseparability of the elastic states (i.e., classical entanglement) [28]. This algorithm determines whether binary functions of two variables, $f(z_1, z_2)$, with both $z_1, z_2 \in 0, 1$, are odd or even. The odd or even character of the function is defined as follows. Since the binary function takes only the values, 0 and 1; there are 16 possibilities. For example, $f(z_1, z_2)$ can take the value 0 or 1 for all $\{z_1, z_2\}$, that is, $f(0,0) = f(0,1) = f(1,0) = f(1,1) = 0$ or $f(0,0) = f(0,1) = f(1,0) = f(1,1) = 1$. These belong to the class of even functions labeled $[0,4]$, $[4,0]$ where the first and second number in the square bracket stand for the number of values of f equal to 1 and 0, respectively. The function can take on one single value of 1; these are functions of the form $f(0,0) = 1, f(0,1) = f(1,0) = f(1,1) = 0$ with all the corresponding permutations of 0s and 1. In this case, the functions are odd and belong to the class $[1,3]$. Functions with two values of 1 (e.g., $f(0,0) = f(0,1) = 1$ and $f(1,0) = f(1,1) = 0$ and the corresponding permutations of 0s and 1s) are even and classified as $[2,2]$. Finally, the permutations of functions with three ones (e.g., $f(0,0) = f(0,1) = f(1,0) = 1$ and $f(1,1) = 0$) are odd and in the class $[3,1]$. Half of the total of 16 possible functions are even or odd. The algorithm addresses the following question: for a given function, how can we determine if it is even or odd? A classic computational approach answers that question by evaluating the function serially for the two possible values of z_1 and z_2. The objective of the quantum-like algorithm is to assess the nature of the function with a single operation using the analogies of superposition and entanglement described in the previous sections. We now use the conventional bra-ket notation of quantum mechanics and apply it to the elastic states of the coupled waveguides. Let $|0\rangle_1 \equiv \vec{e}_1$, $|1\rangle_1 \equiv \vec{e}_2$, $|0\rangle_2 \equiv e^{ikNL}$, and $|1\rangle_2 \equiv e^{ik'NL}$. We note that the four possible inputs of the function $(0,0)$, $(0,1)$, $(1,0)$, $(1,1)$ can be mapped on the basis of the Hilbert space H_{sub}: $|0\rangle_1 |0\rangle_2$, $|0\rangle_1 |1\rangle_2$, $|1\rangle_1 |0\rangle_2$, $|1\rangle_1 |1\rangle_2$. Eq. (14) is now represented as:

$$\vec{V}_N^D = \left(S_{1,1}^D(k, \omega_a) |0\rangle_1 |0\rangle_2 + S_{1,1}^D(k', \omega_b) |0\rangle_1 |1\rangle_2 + S_{1,2}^D(k, \omega_c) |1\rangle_1 |0\rangle_2 + S_{1,2}^D(k', \omega_d) |1\rangle_1 |1\rangle_2\right) e^{i\omega_D t} \tag{16}$$

or

$$\vec{V}_N^D = \left(r_{1,1}^D e^{i\Delta\varphi_1} |0\rangle_1 |0\rangle_2 + r_{1,1}^{D,'} e^{i\Delta\varphi_2} |0\rangle_1 |1\rangle_2 + r_{1,2}^D e^{i\Delta\varphi_3} |1\rangle_1 |0\rangle_2 + r_{1,2}^{D,'} e^{i\Delta\varphi_4} |1\rangle_1 |1\rangle_2\right) e^{i\omega_D t} \tag{17}$$

$r_{1,1}^D$, $r_{1,1}^{D,'}$, $r_{1,2}^D$ and $r_{1,2}^{D,'}$ are the moduli of the complex amplitudes. As mentioned before, Eq. (17) is expressed to within a general phase.

In terms of the representation based on the complex exponentials only (i.e., phases), we prepare the system in the tensor product state:

$$\vec{W}(\omega_D \sim 1.92) = (|0\rangle - |1\rangle)_1 (|0\rangle - |1\rangle)_2 = \begin{pmatrix} 1 \\ -1 \end{pmatrix} \otimes \begin{pmatrix} 1 \\ -1 \end{pmatrix} = \begin{pmatrix} 1 \\ -1 \\ -1 \\ 1 \end{pmatrix}$$

This is done by driving the coupled system at the frequency $\omega_D \sim 1.92$. The algorithm proceeds by invoking an oracle that implements the function f and encodes it into a unitary operation. Each possible function f is encoded by the unitary transformation, U_f, that will act on the prepared state. The unitary transformation is given by:

$$\overleftrightarrow{U}_f = \begin{pmatrix} 1 & 0 & 0 & 0 \\ 0 & -1+2\Sigma & 0 & 0 \\ 0 & 0 & -1+2\Sigma & 0 \\ 0 & 0 & 0 & 1-2\Sigma \end{pmatrix} \tag{18}$$

where $\Sigma = f(0,0) + f(0,1) + f(1,0) + f(1,1)$ modulo 2. $\Sigma = 0$ for the even functions and 1 for the odd one. In the first case, functions in the classes $[0,4], [2,2], [4,0]$, the unitary transformation applied to the prepared state gives

$$\overleftrightarrow{U}_f \vec{W}(\omega_D \sim 1.92) = \begin{pmatrix} 1 & 0 & 0 & 0 \\ 0 & -1 & 0 & 0 \\ 0 & 0 & -1 & 0 \\ 0 & 0 & 0 & 1 \end{pmatrix} \begin{pmatrix} 1 \\ -1 \\ -1 \\ 1 \end{pmatrix} = \begin{pmatrix} 1 \\ 1 \\ 1 \\ 1 \end{pmatrix} = \begin{pmatrix} 1 \\ 1 \end{pmatrix} \otimes \begin{pmatrix} 1 \\ 1 \end{pmatrix}$$

This is a separable state.

In the case of odd functions, in the classes $[1,3], [3,1]$, the unitary operation produces a nonseparable state

$$\overleftrightarrow{U}_f \vec{W}(\omega_D \sim 1.92) = \begin{pmatrix} 1 & 0 & 0 & 0 \\ 0 & 1 & 0 & 0 \\ 0 & 0 & 1 & 0 \\ 0 & 0 & 0 & -1 \end{pmatrix} \begin{pmatrix} 1 \\ -1 \\ -1 \\ 1 \end{pmatrix} = \begin{pmatrix} 1 \\ -1 \\ -1 \\ -1 \end{pmatrix}$$

Note that this later unitary transformation is equivalent to the controlled Z (CZ) gate. Because of the symmetry of the superposition, this operation could be controlled by either bit with the other serving as the target. For instance, the spatial degree of freedoms $\{\vec{e}_1, \vec{e}_2\}$ serve as control bit. The CZ gate acts on the second bit $\{k, k'\}$ only when the first bit is in state , $\vec{e}_2$. Equivalently, we can exchange the roles of $\{\vec{e}_1, \vec{e}_2\}$ and $\{k, k'\}$.

The matrix $\overleftrightarrow{U}_f$ encodes mathematically the physical process of changing the driving frequency. The action of the oracle in implementing the unitary operation, $\overleftrightarrow{U}_f$, results in one of two possible outcomes, the driving frequency of the system is increased either by $\Delta\omega_D = 0.04$ corresponding to the even functions or by $2\Delta\omega_D$ corresponding to the odd functions. Note that the Hermitian conjugate of $\overleftrightarrow{U}_f$, $\overleftrightarrow{U}_f^{\dagger}$ would correspond to a reduction in driving frequency $-\Delta\omega_D$. The sequential application of the transformation and its Hermitian conjugate results in the expected identity as this process corresponds to a frequency that is first up-tuned and then down-tuned by the same amount.

To identify whether a function f is even or odd, one just needs to identify if the final state is separable or nonseparable. The challenge for quantum systems lies now in the measurability of the final states. There is no unambiguous single measurement of entangled states of quantum systems. To distinguish between separable and nonseparable quantum superpositions of states, one needs to make multiple measurements and obtain a statistical representation of the superpositions. However, in the case of elastic waves, the superpositions of states are stable against measurements. For instance, one may detect the separability or nonseparability of the elastic states by employing non-contact methods such as scanning laser Doppler vibrometry which can provide unambiguous information on the wave number as well as the phase of elastic waves supported by the coupled elastic system [22].

6. Implementation of Deutsch-like algorithm exploiting classically entangled elastic states

First, let us consider again the phases of the complex amplitudes of Fig. 3. We now drive the elastic system at three frequencies, ω_D^1, ω_D^2, and ω_D^{ref}. The corresponding phases are labeled, φ_1^1, φ_2^1, φ_3^1, φ_4^1, φ_1^2, φ_2^2, φ_3^2, φ_4^2, and φ_1^{ref}, φ_2^{ref}, φ_3^{ref}, φ_4^{ref}, respectively. The upper script in the phases refer to the driving frequencies. The subscript refers to the same complex amplitudes as Section 5. The system driven at ω_D^{ref} serves as reference. We now encode information in the following 4×1 vector:

$$\Delta\vec{W}^I = \begin{pmatrix} e^{i\left|\varphi_1^I - \varphi_1^{ref}\right|} \\ e^{i\left|\varphi_2^I - \varphi_2^{ref}\right|} \\ e^{i\left|\varphi_3^I - \varphi_3^{ref}\right|} \\ e^{i\left|\varphi_4^I - \varphi_4^{ref}\right|} \end{pmatrix} \tag{19}$$

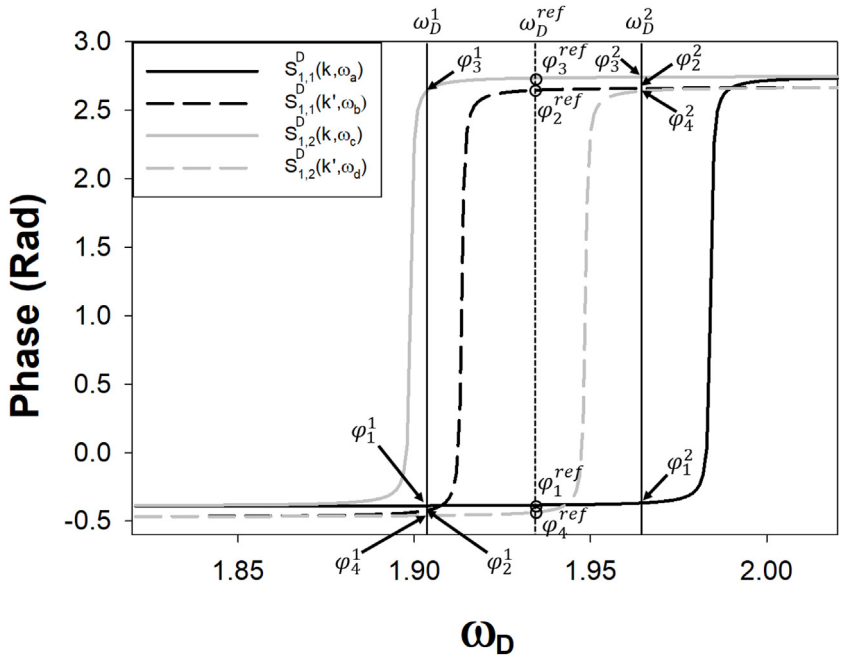

Fig. 4. Phase of the complex amplitudes (Eqs. ((15)a,b,c,d)) as functions of the driving frequency. Physical and geometrical parameters are the same as in Fig. 3. ω_D^1, ω_D^2, and ω_D^{ref} are three possible driving frequencies. The phases of the complex amplitudes corresponding to the reference frequency are indicated by open circles, respectively. The phases corresponding to the driving frequencies ω_D^1, and ω_D^2 are indicated with arrows.

where the upper script I again refers to the driving frequencies 1, 2. This is one of many possible representations of the elastic state of the system for which there will exist a tensor product structure and tensor product basis since all phases involved are also expressible in terms of $\vec{e}_n$ and k and k'.

At the frequency ω_D^1, we have $\Delta\vec{W}^1 = \begin{pmatrix} 1 \\ -1 \\ 1 \\ 1 \end{pmatrix}$ and at the frequency ω_D^2, $\Delta\vec{W}^2 = \begin{pmatrix} 1 \\ 1 \\ 1 \\ -1 \end{pmatrix}$. Both states are nonseparable. They are, however, related to each other through a controlled NOT (CNOT) gate unitary transformation, namely

$$\begin{pmatrix} 1 \\ 1 \\ 1 \\ -1 \end{pmatrix} = \begin{pmatrix} 1 & 0 & 0 & 0 \\ 0 & 0 & 0 & 1 \\ 0 & 0 & 1 & 0 \\ 0 & 1 & 0 & 1 \end{pmatrix} \begin{pmatrix} 1 \\ -1 \\ 1 \\ 1 \end{pmatrix}$$

or

$$\Delta\vec{W}^2 = CX\Delta\vec{W}^1$$

This is a controlled NOT gate CX where the second bit $\{k, k'\}$ serves as control bit. The CX gate acts on the target bit $\{\vec{e}_1, \vec{e}_2\}$ only when the second bit is in state , k'. We can now use this transformation as the primary operation in a variation on the Deutsch algorithm [29].

The objective of this algorithm is to determine if a binary function $f(x)$ defined on the binary domain $x \epsilon \{0, 1\}$ is balanced or constant. The binary function can only take the values 0 or 1. The function is constant if for all x the function takes on the same value, that is, $f(0) = f(1) = 0$ or 1. The function is said to be balanced if $f(0) \neq f(1)$ (i.e., $f(0) = 0$ and $f(1) = 1$ or $f(0) = 1$ and $f(1) = 0$). This is a simplified version of the algorithm developed in Section 6. A classic computation approach would evaluate the function twice serially for the two possible values of x. We seek a quantum-like algorithm that can assess the constant or balanced nature of the function with a single operation (see Fig. 4).

For this, we remap the function $(f(0), f(1)) \rightarrow (g(0), g(1)) = (f(0), |f(0) - f(1)|)$. We reformulate now the problem as that of finding if the function g is balanced or constant.

In a quantum-like algorithm we would prepare the system in a state driven at the frequency ω_D^1, $\Delta\vec{W}^1 = |0\rangle_1|0\rangle_2 + |0\rangle_1|1\rangle_2 + |1\rangle_1|0\rangle_2 - |1\rangle_1|1\rangle_2 \equiv \begin{pmatrix} 1 \\ 1 \\ 1 \\ -1 \end{pmatrix}$ where again $|0\rangle_1, |1\rangle_1$ corresponds to the target bit $\{\vec{e}_1, \vec{e}_2\}$ and $|0\rangle_2, |1\rangle_2$ corresponds to the control bit $\{k, k'\}$.

Given the functions f and g, we map $|x\rangle_1|y\rangle_2$ to $\left|f(y)\bigoplus x\right\rangle_1|y\rangle_2$ where $\bigoplus$ is the addition modulo 2. Therefore if $f(0) = f(1) = 0$, that is $g(0) = g(1) = 0$ (g is constant), then the prepared state remains the same $\Delta\vec{W}^1$ after transformation. If $f(0) = 0$ and $f(1) = 1$ that is $g(0) = 0$ and $g(1) = 1$ (g is balanced), then the prepared state transforms to $|0\rangle_1|0\rangle_2 + |1\rangle_1|1\rangle_2 + |1\rangle_1|0\rangle_2 - |0\rangle_1|1\rangle_2 \equiv \begin{pmatrix} 1 \\ -1 \\ 1 \\ 1 \end{pmatrix}$.

If $f(0) = 1$ and $f(1) = 0$ that is $g(0) = 1$ and $g(1) = 1$ (g is constant), then the prepared state transforms into itself. If $f(0) = 1$ and $f(1) = 1$ that is $g(0) = 1$ and $g(1) = 0$ (g is balanced), then the prepared state transforms to $|1\rangle_1|0\rangle_2 + |1\rangle_1|1\rangle_2 + |0\rangle_1|0\rangle_2 - |0\rangle_1|1\rangle_2 \equiv \begin{pmatrix} 1 \\ -1 \\ 1 \\ 1 \end{pmatrix}$. The unitary transformations corresponding to these four cases are therefore the identity matrix if g is constant and the CX operation if g is balanced. From a practical point of view, an oracle would apply these transformations by not changing the driving frequency of the prepared state if the function g is constant and up-tuning the frequency of the driver to ω_D^2 in the case of a balanced function. Since the prepared and transformed nonseparable superpositions are elastic states, they can be experimentally examined without further application of quantum gate operations as is necessary in a true quantum algorithm.

7. Conclusion

We have presented Deutsch-like and Deutsch–Jozsa-like algorithms which involve "classical entanglement" that can be implemented on classical systems composed of a planar array of two finite one-dimensional discrete elastic waveguides mutually coupled periodically along their length and driven externally. The elastic modes of this system have been analyzed in detail and shown to be products of states associated with degrees of freedom along (Bloch modes) and across the waveguides (spatial modes). Superpositions of product states of the periodically coupled waveguides analogous to those of a two partite system composed of two two-level elastic bits can be generated by application of an external driver. The driver's frequency and amplitudes serve as tuning parameters to navigate the Hilbert space of product states. The Deutsch–Jozsa-like quantum-like algorithm can distinguish between the even or odd character of all possible binary functions for two elastic bits inputs. The Deutsch-like algorithm distinguishes between constant and balance binary functions. The algorithms presented here solve these problems in a single operation by using the nonseparability (i.e., the parallelism) of the superpositions of product states of the periodically coupled waveguides. At the core of these algorithms are two controlled unitary operations, a controlled Z gate (CZ) and a controlled NOT gate (CX). The advantage of using nonseparable superpositions of elastic states, is that they can be examined directly via contact ultrasonic methods (e.g., transducers) [21] or non-contact methods (e.g., scanning laser Doppler vibrometry) [22]. From a practical point of view, the discrete coupled elastic system studied theoretically in this paper could be physically realized by using finite continuous one-dimensional rod-like elastic waveguides coupled along their length with an elastically stiff adhesive such as epoxy. A periodic arrangement of segments of the adhesive between the rod-like waveguides will enable periodic coupling leading to the desired band folding [24]. Ultrasonic transducers attached to the detection end of the finite length rod-like waveguides will enable measurement of the relative phase between the waveguides. The laser Doppler vibrometer will enable the mapping of the longitudinal displacement field along the rod-like waveguides [22]. Fourier transformation in space of the spatial waveform enables the determination of the wave number associated with each mode of oscillation. These measurements can then be used to extract the complex amplitudes in the expansion of the displacement field given by Eqs. (14) and (16) and therefore, determine their associated phase.

The algorithms described here exploit discrete jumps in the phase (or differences between phases) of resonances. By increasing dissipation, the bandwidth of the resonances will increase giving access to a variety of choices of the value of phases by tuning the driving frequency. This will provide access to phase shift gates, a necessary feature in quantum Fourier Transform algorithms [30]. Furthermore, while we have considered here, algorithms that can be performed on two elastic bits, we note that the form of Eq. (13) may enable navigation of the Hilbert space of a three-bit elastic system. Extension to larger numbers of bits, will require elastic systems that can support larger numbers of degrees of

freedom or exhibit nonlinear elasticity. Maximally entangled exponentially complex superpositions of nonlinear product states in externally driven arrays of nonlinear waveguides have been demonstrated theoretically [31]. The phase of the complex resonant amplitudes of the superposition of nonlinear product states can then be used in manners similar to those described in this paper to expand the capability and scalability of arrays of elastically coupled waveguides for quantum-like information processing.

Finally, the recent emergence of topological acoustics enables us to foresee all-acoustic information processing platforms that go beyond the canonical attributes of sound wave frequency, wave vector and dynamical phase by embracing the realm of the geometric phase [32–34]. For example, periodic topological elastic systems may support bands with "quantized" geometric phase (e.g., Berry phase). This quantization suggests that such elastic system may lead to analogies with true quantum mechanical systems. It may, therefore, be possible to employ and control the geometric phase to encode information similarly to that encoded in emerging quantum information storage and processing devices [35]. In addition, symmetry breaking in acoustic topological insulators creates Dirac-like physics such as pseudospin degrees of freedom and topologically protected edge states. Pseudospin dependent edge modes can propagate unidirectionally along interfaces between structurally differing domains with different topological characteristics (i.e., domains with different geometric phases). For instance, interfaces between tunable structures of honeycomb-lattice sonic crystals have been reconfigured to program the propagation path of acoustic edge modes and realize acoustic switches and tunable logic gates [36,37]. Acoustic topological insulators exhibit robust properties with respect to a variety of structural changes potentially providing flexibility in the design of a wide range of acoustic logic elements.

Declaration of competing interest

The authors declare that they have no known competing financial interests or personal relationships that could have appeared to influence the work reported in this paper.

Data availability statement

The data that support the findings of this study are available from the corresponding author upon reasonable request.

Acknowledgments

This work was supported in part by a grant from the W.M. Keck foundation and by National Science Foundation Emerging Frontiers in Research and Innovation (EFRI), United States of America award # 1640860.

References

[1] M. Serra-Garcia, Turing-complete mechanical processor via automated nonlinear system design, Phys. Rev. E 100 (2019) 042202.
[2] S. Bringuier, N. Swinteck, J.O. Vasseur, J.-F. Robillard, K. Runge, K. Muralidharan, P.A. Deymier, Phase-controlling phononic crystals: Realization of acoustic boolean logic gates, J. Acoust. Soc. Am. 130 (2011) 1919.
[3] T. Zhang, Y. Cheng, B.-G. Yuan, J.-Z. Guo, X.-J. Liu, Compact transformable acoustic logic gates for broadband complex boolean operations based on density-near-zero metamaterials, Appl. Phys. Lett. 108 (2016) 183508.
[4] F. Li, P. Anzel, J. Yang, P.G. Kevrekidis, C. Daraio, Granular acoustic switches and logic elements, Nature Commun. 5 (2014) 5311.
[5] M. Porter, P. Kevrekidis, C. Daraio, Granular crystals: Nonlinear dynamics meets materials engineering, Phys. Today 68 (11) (2015) 44.
[6] J.P. Dowling, G.J. Milburn, Quantum technology: The second quantum revolution, Phil. Trans. R. Soc. A 361 (2003) 1655.
[7] R. Jozsa, N. Linden, On the role of entanglement in quantum-computational speed-up, Proc. R. Soc. Lond. Ser. A Math. Phys. Eng. Sci. 459 (2003) 2011.
[8] K. Cheng, W. Zhang, Z. Wei, Y. Fan, C. Xu, C. Wu, X. Zhang, H. Li, Simulate Deutsch-Jozsa algorithm with metamaterials, Opt. Express 28 (2020) 16230.
[9] W. Zhang, K. Cheng, C. Wu, Y. Wang, H. Li, X. Zhang, Implementing quantum search algorithm with metamaterials, Adv. Mater. 30 (2018) 1703986.
[10] B. Perez-Garcia, R.I. Hernandez-Aranda, A. Forbes, T. Konrad, The first iteration of Grover's algorithm using classical light with orbital angular momentum, J. Modern Opt. 65 (2018) 1942.
[11] T.W. Hijmans, T.N. Huussen, R.J.C. Spreeuw, Time- and frequency-domain solutions in an optical analogue of Grover's search algorithm, J. Opt. Soc. Amer. B 24 (2007) 214.
[12] G. Puentes, C. La Mela, S. Ledesma, C. Iemmi, J.P. Paz, M. Saraceno, Optical simulation of quantum algorithms using programmable liquid-crystal displays, Phys. Rev. A 69 (2004) 042319.
[13] N. Bhattacharya, H.B. van Linden van den Heuvell, R.J.C. Spreeuw, Implementation of quantum search algorithm using classical Fourier optics, Phys. Rev. Lett. 88 (2002) 137901.
[14] R.J.C. Spreeuw, A classical analogy of entanglement, Found. Phys. 28 (1998) 361.
[15] P. Ghose, A. Mukherjee, Entanglement in classical optics, Rev. Theor. Sci. 274 (2014).
[16] E. Karimi, R.W. Boyd, Classical entanglement? Science 350 (2015) 1172.
[17] E. Otte, I. Nape, C. Rosales-Guzmán, A. Vallés, C. Denz, A. Forbes, Recovery of nonseparability in self-healing vector bessel beams, Phys. Rev. A 98 (2018) 053818.
[18] S.M. Hashemi Rafsanjani, M. Mirhosseini, O.S. Magaña Loaiza, R.W. Boyd, State transfer based on classical nonseparability, Phys. Rev. A 92 (2015) 023827.
[19] L.J. Pereira, A.Z. Khoury, K. Dechoum, Quantum and classical separability of spin–orbit laser modes, Phys. Rev. A 90 (2014) 053842.
[20] M. McLaren, T. Konrad, A. Forbes, Measuring the nonseparability of vector vortex beams, Phys. Rev. A 92 (2015) 023833.
[21] M. Arif Hasan, L. Calderin, T. Lata, P. Lucas, K. Runge, P.A. Deymier, The sound of bell states, Nat. Commun. Phys. 2 (2019) 106.

[22] M.Arif. Hasan, L. Calderín, T. Lata, P. Lucas, K. Runge, P.A. Deymier, Experimental demonstration of elastic analogues of nonseparable qutrits, Appl. Phys. Lett. 116 (2020) 164104.
[23] P.A. Deymier, K. Runge, M.A. Hasan, Exponentially complex nonseparable states in planar arrays of nonlinearly coupled one-dimensional elastic waveguides, J. Phys. Commun. 4 (2020) 085018.
[24] P.A. Deymier, M.A. Hasan, K. Runge, Navigating the Hilbert space of nonseparable elastic states in arrays of periodically coupled one-dimensional waveguides, AIP Adv. 10 (2020) 095101.
[25] P. Zanardi, Virtual quantum subsystems, Phys. Rev. Lett. 87 (2001) 077901.
[26] P. Zanardi, D.A. Lidar, S. Lloyd, Quantum tensor product structures are observable induced, Phys. Rev. Lett. 92 (2004) 060402.
[27] D. Deutsch, R. Jozsa, Rapid solutions of problems by quantum computation, Proc. R. Soc. Lond. Ser. A Math. Phys. Eng. Sci. 439 (1992) 553.
[28] K.D. Arvind, N. Mukunda, A two-qubit algorithm involving quantum entanglement, 2000, arXiv:quant-ph/0006069.
[29] D. Deutsch, Quantum. Theory, The Church-Turing principle and the universal quantum computer, Proc. R. Soc. Lond. Ser. A Math. Phys. Eng. Sci. 400 (1985) 97.
[30] M. Nielsen, I. Chuang, Quantum Computation and Quantum Information, Cambridge University Press, Cambridge, 2000.
[31] P.A. Deymier, K. Runge, M.A. Hasan, Exponentially complex nonseparable states in planar arrays of nonlinearly coupled one-dimensional elastic waveguides, J. Phys. Commun. 4 (2020) 085018.
[32] P.A. Deymier, K. Runge, Sound Topology, Duality, Coherence and Wave-Mixing: An Introduction to the Emerging New Science of Sound, in: Springer Series in Solid-State Sciences, vol. 188, 2017.
[33] Z.J. Yang, F. Gao, X.H. Shi, et al., Topological acoustics, Phys. Rev. Lett. 114 (2015) 114301.
[34] R. Fleury, A. Khanikaev, A. Alu, Floquet topological insulators for sound, Nat. Comm. 7 (2016) 11744.
[35] A. Ehert, M. Ericson, P. Hayden, H. Inamori, J.A. Jones, D.K.L. Oi, V. Verdal, Geometric quantum computation, J. Modern Opt. 47 (2000) 2501.
[36] H. Pirie, S. Sadhuka, J. Wang, J.E. Hoffman, Topological Phononic Logic, arXiv:1809.09187.
[37] J.-P. Xia, D. Jia, H.-X. Sun, S.-Q. Yuan, Y. Ge, Q.-R. Si, X.-J. Liu, Programmable coding acoustic topological insulator, Adv. Mater. 30 (2018) 1805002.